Investigation on Metaradiator based on Metasurface

Sarawuth Chaimool

Electrical Engineering and Electronics Technology, Faculty of Technology, Udon Thani Rajabhat University, Thailand
Email: jaounarak@gmail.com

Tanan Hongnara[a] and **Prayoot Akkaraekthalin**[b]

Electrical and Computer Engineering, Faculty of Engineering, King Mongkut's University of Technology North Bangkok, Thailand
Email: tanan.hongnara@hotmail.com[a] and prayoot@kmutnb.ac.th[b]

Manuscript received September 28, 2015
Revised October 27, 2015

ABSTRACT

Three unusual electromagnetics properties of metasurface namely negative permittivity (ENG), negative permeability (MNG), and near-zero refraction index (NZI) have been investigated. These properties are obtained by coupling effect of the combination between fractal fishnet structure and closed ring resonator on different sides of unit cell. To better understand the characteristics of metasurface, the metasurface as a superstrate/cover placed atop a conventional dipole at a small distance, which called metaradiator, has been studied and demonstrated. Moreover, in order to understand and explain clearly the unusual behaviors of metasurface, the robust retrieval method and the generalized sheet transition conditions have been applied to extract effective material properties. Numerical and simulated results show three different radiation patterns of metaradiator are strongly affected from metasurface within the entire band.

Keywords: *metamaterial, metasurface, metaradiator, ENG, MNG, NZI*

1. INTRODUCTION

Nowadays, the design and engineering of artificial composite structures named as Metamaterial have sparked exponentially increased rapidly. Many phenomena and applications of metamaterials are related to perfect imaging [1], invisible cloak [2], electromagnetic (EM) wave perfect absorbers [3], enhanced efficiency of antenna [4] - [5], zero-ordered antenna [6], microwave filter [7] and artificial magnetic permeability [8]. As the typical building blocks of metamaterials, the split ring resonator (SRR) and the wire rod have been studied [9]. Their local resonances are supported by both metallic structures endow them with role of electric and magnetic meta-atoms in constructing metamaterials of the wire rod and SRR, respectively [10]. Besides, they have desired bulk EM behavior, therefore, metasurface or metafilm has been suggested and extended from three-dimension (3D) to a two-dimension (2D) pattern at a planar surface [11]. The metasurface is a 2D version of the bulky metamaterial structure which takes less physical space and offers a less lossy structure for possible artificial control of electromagnetic waves through it. As a new area of research, the cutting edge technology may lift up the designing and realization of metasurface towards novel functionalities and improved performance inclusion which may facilitate obtaining increased bandwidths and reduced losses. These properties make metasurface able be applied to microwave circuits and antennas.

Due to their intrinsic structures, the conventional wire rod and SRR cannot give the rise to a significant ratio of the operating wavelength over their sizes. Moreover, it is well known that significantly subwavelength electromagnetic resonators have been employed in antennas and microwave circuit applications. In order to realize the high-performance metasurfaces, these meta-atoms or unit cells should be made as subwavelength as possible [12]. Over a few years, fractal techniques have been widely used in the design of frequency selective surface and metamaterials. Due to their self-similar property, the fractal based metamaterials offer multiband operations. Also, since their space filling property, they can be used to miniaturize the dimension of unit cell.

In this paper, we have investigated experimentally

and numerically the electromagnetic characteristics of the combination between Minkowski fractal fishnet structure and closed ring resonator as metasurface in the microwave frequency range. The fractal scheme employed in this research is from the viewpoint of a much electrically smaller unit cell of metasurface in virtue of the space-filling properly. Combining two types of resonators formed the metasurface, it has ENG, MNG and NZI characteristics. In addition, we also interpret the bulk permittivity and permeability to 2D effective electric and magnetic surface susceptibilities. In order to better understand metasurface behaviors by putting a simple dipole antenna closed to metasurface, we find that the antenna's radiation patterns have different peaks of main beams independently-controlled frequencies.

2. CHARACTERIZATIONS OF METASURFACE

During the recent years, several methods have been proposed to extract the effective material properties of metamaterial slab [12] - [13]. Some researchers have concentrated their work on easy and robust retrieval method for effective constitutive parameters (permittivity, permeability and refractive index) to characterize the metamaterial and metasurface. These techniques are generally based on the inversion of the reflection and transmission parameters of a normally incident wave on the slab. After obtaining the wave impedance (z) and effective refractive index (n), the scalar values of effective permittivity (ε_{eff}) and effective permeability (μ_{eff}) are then calculated as $\mu_{eff}= n*z$ and $\varepsilon_{eff}= n/z$. However, electromagnetic behavior of most metamaterial designs is anisotropic or bi-anisotropic, which require a tensor for characterizing it. The recent technique developed by Szabo *et. al.* is based on Kramers-Kronig relations and thus complied with the principle of causality [14]. While the conventional methods to model 3D-metamaterials is with effective medium theory [12] - [14], the characterization of metasurfaces was suggested to use other ways [11], [16]-[19] due to its planar surface nature. The reason is that no unique values of effective material properties can be obtained as they depend on the value of effective thickness. One of the promising techniques for metasurface is the application of the generalized sheet transition conditions (GSTCs) [17], where the averaged boundary conditions are applied for the specular interaction of electromagnetic waves with a surface of electrically small scatterers. The electric and magnetic surface susceptibilities, which associate the EM field response to the surface polarization densities of the scatterers at the metasurface [18]. In this paper, we used both methods including robust method [14] and GSTCs) [17] to compare and explain the characteristics of the proposed metasurface. In this particular design, the metasurface is illuminated by a normally incident plane electromagnetic wave with E-polarization in the x direction as shown in Fig. 1. The proposed unit cell consists of two resonator types of resonators namely closed ring resonator and fractal fishnet structure on two sides of square area of 18×18 mm^2. On the top side, the second-iteration order of Minkowski geometry is applied as depicted in Fig. 1. The Minkowski fractal fishnet of the second-iteration order is utilized by taking a trade-off between miniaturization and fabrication. On another side, a square closed ring resonator with the patch is used as shown in Fig. 1. The advantage of this unit cell is supporting two linear orthogonal polarizations and also the capability of independent control of permeability and permittivity of the bands that unusual characteristics. Computations were performed with a commercial full-wave software (CST Microwave Studio).

By studying the commonly used effective parameter extraction techniques, the effective constitutive parameters, permeability (μ_{eff}) and permittivity (ε_{eff}) are extracted; the graphical presentation is given in Figure 2(a). It is observed the effective ε_{eff} response that it is form Drude model [10] with $\varepsilon_{eff}= 1-(\omega_p^2/\omega)$, where ω_p is the electric plasma frequency with ε_{eff} equal zero value. Also, due to high Q of permittivity, the obtained characteristic rapidly changes through plasma frequency of 1.24 GHz with extreme high slope. Meanwhile, the magnetic plasma frequency is 1.27 GHz from effective constitutive permeability. This characteristic response is well known that Lorentz dispersive model [10]. It means that each side of metasurface contains a periodic structure producing one of the resonant plasma frequencies. From above results, it can be classified that the epsilon negative (ENG) behavior is the real part of ε_{eff} has negative values while μ_{eff} is positive. The ENG frequency range is below 1.24 GHz. At the center of the refractive index response, it has near zero value of the refractive index (NZI) that is perceived at frequency around 1.25 GHz. Vice versa, the frequency range above 1.27 GHz is claimed with negative value (MNG) of μ_{eff} whereas ε_{eff} has positive values.

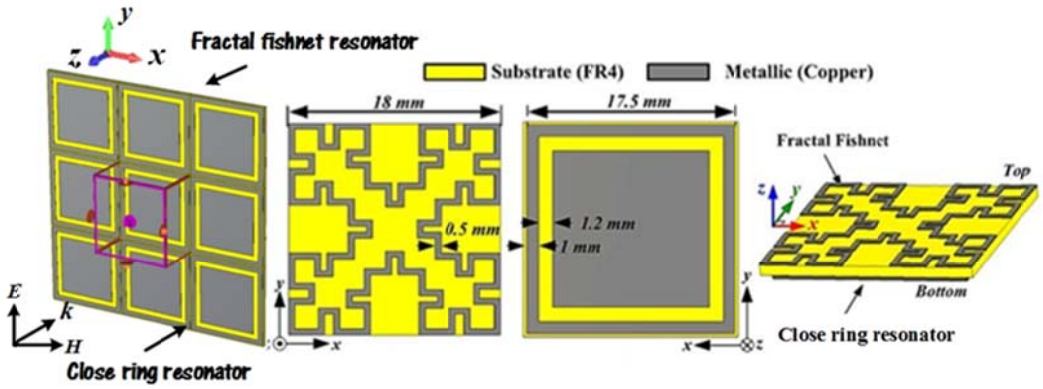

Fig. 1 *Configuration and dimensions of the proposed metasurface. Metasurface is printed on FR-4 substrate with* ε_r *= 4.2 and thickness of 0.8 mm.*

In another point of view, the electric and magnetic susceptibility parameters are extracted by using set of equations [17] as shown in Fig. 2(b) and 2(c), where effective electric and magnetic surface susceptibilities are symbolical as χ_{ES} and χ_{MS}, respectively. The parameters χ_{ES} and χ_{MS} are the dyadic surface electric and magnetic susceptibilities that related the electric and magnetic polarizability densities of the scatterers per unit area. It is clearly seen that χ_{ES} and χ_{MS} are virtually the same as the effective ε_{eff} and μ_{eff} (Fig. 2(a)) with different positive and negative scales, respectively. It is seen that a strong electric resonance occurs at 1.24 GHz compared with the magnetic response. The real part of χ_{MS} becomes positive above the plasma frequency. A positive magnetic surface susceptibility χ_{MS} is obtained above 1.27 GHz for this perfect electric conductor scatterer. This implies a correct polarity for χ_{MS} at which *diamagnetic materials* was defined in [20].

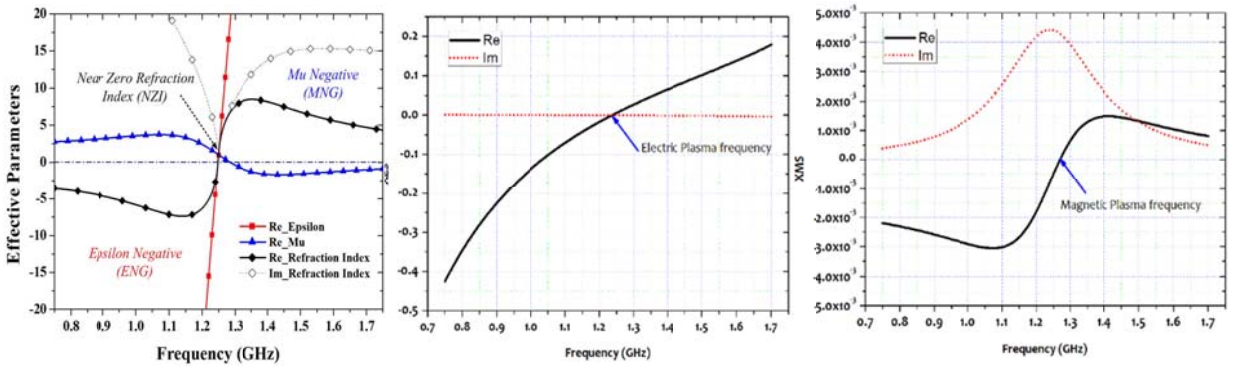

(a) (b) (c)

Fig. 2 *(a) Effective constitutive parameters using robust retrieval method and Generalized sheet transition conditions (GSTCs) (b) effective electric surface susceptibility (*χ_{ES}*) and (c) magnetic surface susceptibility (*χ_{MS}*).*

3. RESULTS AND DISCUSSION

To investigate and better understand the unusual behaviors of the proposed metasurface, we placed a simple half-wavelength dipole as primary source closed to the metasurface. The metasurface consists of 25 unit cells in a 5×5 arrangement. The cross-sectional view and detailed view of the proposed antenna with its optimized parameters are presented in Fig. 3(a). For this obtained coordinate, the dipole has omnidirectional pattern around *y*-axis. Actually, to guarantee the bandwidth of the final antenna, both the metasurface and dipole

should operate in a wideband with fully overlapped frequencies. However, in order to ensure that the primary source has only the first mode with omnidirectional pattern. Therefore, three dipoles with different resonant frequencies at 1.15 GHz, 1.29 GHz, and 1.40 GHz have been designed. $|S_{11}|$ and radiation patterns are shown in Fig. 3(b). It can be seen that all three resonant frequencies have omnidirectional patterns with gain of 2.0 dBi. Then, place the metasurface closed to dipole where the closed ring resonators are faced to the dipole. The simulated normalized radiation patterns at 1.15 GHz, 1.29 GHz, and 1.40 GHz are plotted in Fig. 4. The three distinct modes have different radiation pattern characteristics as the location of peaks in the 3-D radiation patterns change. As expected, the radiation patterns of each frequency are dramatically affected by the presence closely spaced metasurface in its near-field region. It is evident that the proposed metasurface can work at 1.29 GHz as a transparent surface (reflectionless), frequency ranges below 1.29 GHz as reflector and above 1.29 GHz as a director-like providing a phenomenon of anomalous reflection. It can be explained that this director-like property makes it possible to use an external source to drive a surface current on the resonator structure, so as to interfere with the current induced by the primary incident wave, leading to changes in the far field radiation pattern.

It is concluded that metasurface can reflect the incident wave in anomalous way or control the propagation of the incident wave. Generally speaking, the antenna can switch its radiation without any switch. For most of the metasurface's in the literature, unfortunately, it is not possible to control the bands independently or arbitrarily. For instance, for the metasurface's employing permeability near zero (MNZ) was used in desired band [4].

4. CONCLUSION

To conclude, we have succeeded through both theory and experiment that different kinds of unusual behaviors of metasurface can serve different beam directions as subwavelength reflector, transparent surface and director-like surface. As a specific demonstration, a dipole with metasurface is able to control its radiation pattern with different maximum beam directions depending on the unusual behaviors of metasurface. As results, the proposed metasurface will open a new way to control the radiation pattern, promising great potentials in modern wireless communication systems especially cognitive radios. Moreover, with geometrical scalability, this concept can be further applied to millimeter-wave or optical regimes.

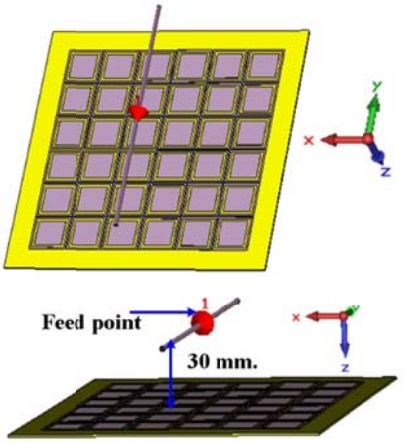

(a)

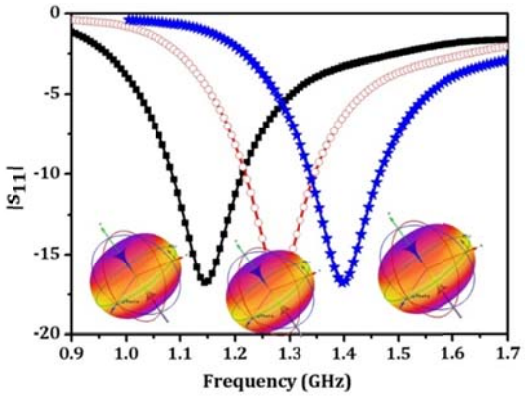

(b)

Fig. 3 *(a) Configuration of the dipole with metasurface and (b) $|S_{11}|$ and radiation patterns of the dipoles alone with different frequencies.*

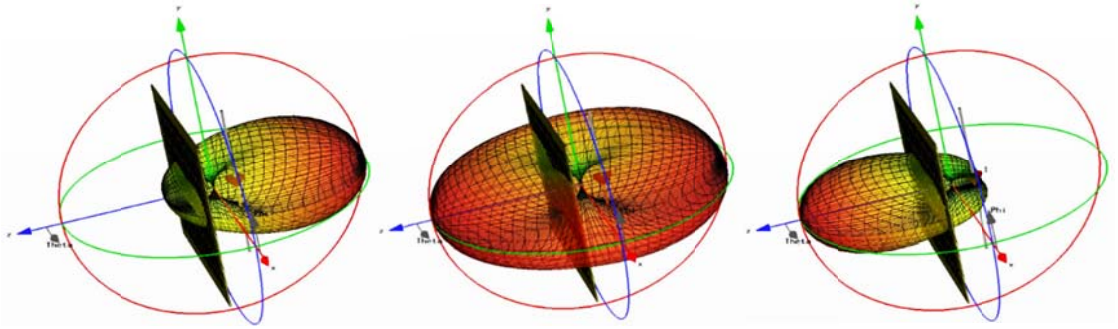

(a) (b) (c)

Fig. 4 *Simulated 3–D radiation patterns (a) 1.15 GHz with ENG, (b) 1.29 GHz with NZI and (c) 1.40 GHz with MNG.*

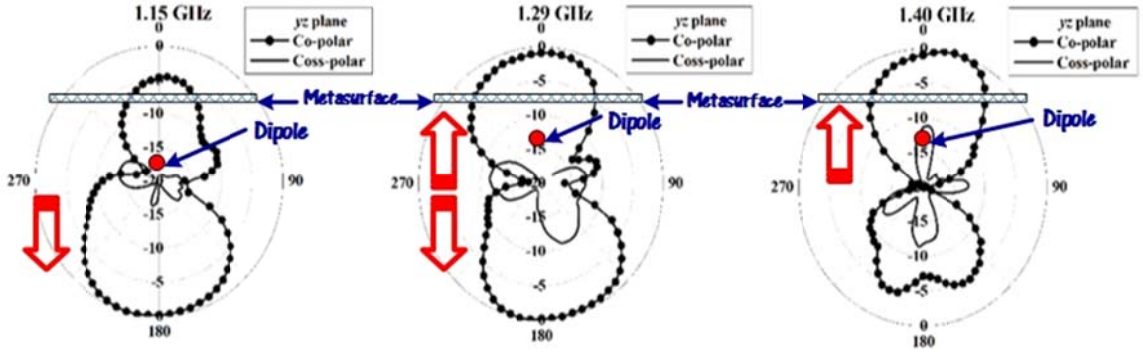

(a) (b) (c)

Fig. 5 *Measured radiation patterns (a) 1.15 GHz with ENG, (b) 1.29 GHz with NZI and (c) 1.40 GHz with MNG.*

5. ACKNOWLEDGEMENTS

This work has been supported by the Thailand Research Fund (TRF) through the TRF Senior Research Scholar Program Grant No. RTA5780010).

REFERENCES

[1] J. B. Pendry, "Negative refraction makes a perfect lens," *Phys. Rev. Lett.,* vol. 85, no. 3966, 2000.

[2] D. Schurig, J. J. Mock, B. J. Justice, and S. A. Cummer, J. B. Pendry, A. F. Starr, D. R. Smith, "Metamaterial electromagnetic cloak at microwave frequencies," *Science*, vol. 314, no. 5801, pp. 977-980, Nov. 2006.

[3] N. I. Landy, S. Sajuyigbe, J. J. Mock, D. R. Smith, and W. J. Padilla, "Perfect metamaterial absorber," *Phys. Rev. Lett*., vol. 100, no. 20, pp. 207402-5, May 2008.

[4] S. Chaimool, C. Rakluea, and P. Akkaraekthalin, "Mu-Near-Zero metasurface for microstrip-fed slot antennas," *Applied Physics A*, vol. 112, pp. 669-675, 2013.

[5] S. Chaimool, Kwok L. Chung, and P. Akkaraekthalin, "Simultaneous gain and bandwidth enhancement of a single-feed circularly polarized microstrip patch antenna using a matamaterial reflective surface," *Progress In Electromagnetics Research* B, vol.22, pp.23-37, 2010.

[6] S. Chaimool, T. Pechrkool, K. L. Chung, and P. Akkaraekthalin, "A compact zeroth-order resonant antenna based on modified Jerusalem cross mushroom structure" , in *Proc. Inter. Workshop on Antenna Tech.*, pp. 377-379, 201

[7] S. Chaimool and P. Akkaraekthalin, "Miniaturized wideband bandpass filter with wide stopband using metamaterial-based resonator and defected ground structure," *RadioEngineering*, vol. 2, pp. 611-616, June 2012.

[8] S. Chaimool, A. Pinsakul, and P. Akkaraekthalin, "Patch antenna miniaturization using artificial magneto-dielectric metasubstrate," in *Proc. Inter. Conf. of Intern Symp. on Antennas Propag.*, pp. 906-909, 2012.

[9] N. Engheta and R.W. Ziolkowski, "Electromagnetic metamaterials: physics and engineering explorations," *John Wiley & Sons, Hoboken*, NJ, 2006.

[10] S. Chaimool, T. Hongnara, and P. Akkaraekthalin, "Low and zero refractive index metamaterials: characteristics and its

applications," in *Proc. Inter. Electrical Engineering Congress,* pp. 217-220, 2013.
[11] C. L. Holloway, E. F. Kuester, J. A. Gordon, J. O'Hara, J. Booth, and D. R. Smith, "An overview of the theory and applications of metasurfaces: The two-dimensional equivalents of metamaterials," *IEEE Antennas Propag. Mag.,* vol. 54, no. 2, pp. 10–35, Apr. 2012,
[12] S. N. Burokur, R. Yahiaoui, and A. de Lustrac, "Subwavelength resonant cavities fed by microstrip patch array," in *Proc. IEEE Int. Workshop Antenna Technology*, Mar. 2–4, 2009, pp. 1–4.
[13] X. Chen, B. I. Wu, L. Ran, T. M. Grzegorczyk, and J. A. Kong, "Robust method to retrieve the constitutive effective parameters of metamaterilas," *Phys. Rev. E*, vol. 70, pp.0166081-0166087, 2004.
[14] C. Menzel, C. Rockstuhl, T. Paul, F. Lederer, and T. Pertsch, "Retrieving effective parameters for metamaterials at oblique incidence," *Phys. Rev. B,* vol. 77, Apr. 2008.
[15] Z. Szabo, G. H. Park, R. Hedge, and E. P. Li, "A unique extraction of metamaterial parameters based on Kramers-Kronig relationship," *IEEE Trans. Microw. Theory Tech.*, vol. 58, no. 10, pp. 2224–2230, Oct. 2010.
[16] D. Morits and C. Simovski, "Electromagnetic characterization of planar and bulk metamaterials: A theoretical study," *Phys. Rev. B*, vol. 82, p. 165114, 2010.
[17] C. L. Holloway, E. F. Kuester, and A. Dienstfey, "Characterizing metasurfaces/meta films: The connection between surface susceptibilities and effective material properties," *IEEE Antennas Wireless Propag. Lett.,* vol. 10, no. , pp. 1507–1511, 2011.
[18] C. L. Holloway, D. Love, E. F. Kuester, J. A. Gordon, and D. A. Hill, "Use of generalized sheet transition conditions to model guided waves on metasurfaces/meta films," *IEEE Antennas Propag* ., vol. 80, no. 11, pp. 5173–5186, Nov. 2012.
[19] A. I. Dimitriadis, N. V. Kantartzis, I. T. Rekanos, and T. D. Tsiboukis, "Efficient Metafilm/Metasurface characterization for obliquely incident TE waves via surface susceptibility models," *IEEE Trans. Magn.,* vol. 48, no. 2, pp. 367–370, Feb. 2012
[20] C. L. Holloway, D. C. Love, E. F. Kuester, A. Salandrino, and N. Engheta, "Sub-wavelength resonators: On the use of metafilms to overcome the λ/2 size limit," *IET Microw. Antennas Propag.*, vol. 2, pp. 120–129, 2008.

Sarawuth Chaimool, photograph and biography not available at the time of publication.

Tanan Hongnara, photograph and biography not available at the time of publication.

Prayoot Akkaraekthalin, photograph and biography not available at the time of publication.